

NUMERICAL PREDICTION OF MASSIVE SEPARATION AND UNSTEADY FLOWS AROUND BLUFF-BODIES

Zhixiang Xiao

School of Aerospace
Tsinghua University

No.1, Qing Hua Yuan, Haidian District, Beijing, China, 100084
xiaotigerzhx@tsinghua.edu.cn

Jian Liu

School of Aerospace
Tsinghua University

No.1, Qing Hua Yuan, Haidian District, Beijing, China, 100084
liujian08@mails.tsinghua.edu.cn

Song Fu

School of Aerospace
Tsinghua University

No.1, Qing Hua Yuan, Haidian District, Beijing, China, 100084
fs-dem@tsinghua.edu.cn

ABSTRACT

The massively separated unsteady flows are numerically simulated by DDES based on $k-\omega$ -SST model. The original dissipation is multiplied by a function, which is less and equal to 1, to effectively reduce the effect of numerical dissipation in the recirculation region. A very important parameter in DDES, C_{DES} , is recalibrated using decaying of isotropic turbulence. Two cases are simulated, where one is NACA0021 at incidence of 60 degrees and another is tandem-cylinders. In the first case, the effect of spanwise length is investigated and longer spanwise length can obtain better results; in the second case, the fully turbulent and quasi-laminar assumptions are both applied to predict the flow. The quasi-laminar assumption performs like the trip in the experiment and it can improve the results, such as velocity, TKE, and so on, in a certain extent.

INTRODUCTION

Unsteady and massively separated flows around bluff bodies, such as tandem cylinders (TC) (Jenkins et al., 2005; Jenkins et al., 2006 and Neuhart et al., 2009), are very complicated and three-dimensional (3-D). This kind of massive separation greatly challenges the turbulence prediction methods, and almost no turbulence model in Reynolds-averaged Navier-Stokes (RANS) solver can well

predict the unsteady flow characteristics and mechanism of interaction between vortices and components.

The poor performance for massive separation using turbulence models has motivated the increasing investigation of large eddy simulation (LES). LES is well known to directly resolve the large-scale structures and only to model the small-scale structures. It is thus a powerful tool, providing a description of large, energy-containing scales of motion that are typically dependent on geometry and boundary conditions. The small-scale motion is thought as nearly homogeneous and is easily to be modeled. However, when LES is applied to boundary layers at high Reynolds number, the computation cost of whole-domain LES does not differ significantly from that of direct numerical simulation. The “large eddies” approaching to the solid wall are physically small in scale. LES requires additional empiricism in the treatment of boundary layer. Furthermore, the subgrid scale models for the boundary layer flows are not mature and need further improvement. If LES is hoped to accurately predict the flow in engineering (Re about 10^6), it will be achieved in several decades later (Spalart, 2000).

RANS/LES hybrid methods contain advantages of both RANS and LES. Such hybrid methods combine a high-efficiency turbulence model near the wall where the main flow features are dominated by small-scale turbulent fluctuations with a LES-type treatment for the large-scale motion in the core flow region far away from the wall. It can be thought as a

high efficient and high accuracy turbulence modeling methods for prediction of unsteady flows at high Reynolds numbers.

Detached eddy simulation (DES, Spalart, 1997) is a widely used RANS/LES hybrid method. However, the unphysically separations in the boundary layer can be observed due to the locally clustering grids. The computational results are sensitive to the grids density and distribution. Then, the delayed-DES (DDES, Spalart et al., 2006; Menter et al., 2003; Fu et al. 2007; Xiao et al., 2006 and 2009) is applied to predict the massive separation flows past bluff bodies.

In fact, the numerical dissipation also has an important influence on both time-averaged and instantaneous results. Strelets (2001) proposed a function ranging from 0 to 1 automatically in the spatial scheme. The function approaches to 0 in the recirculation region and approaches to 1 near the wall and in the irrotational region where the mesh is not enough dense. This function is also implemented and validated in our in-house code.

In this article, decaying of isotropic turbulence (DIT) is firstly used to validate our in-house code and to recalibrate the important parameter, C_{DES} . Then, two cases of NACA0021 at incidence of 60 degrees (Werner et al., 2009) and tandem cylinders (TC), are simulated using the turbulence modeling methods. The computational results are compared with available measurements to present the capabilities of DDES with adaptive dissipation. Furthermore, influence of spanwise length and quasi-laminar (QL) assumption would be analyzed.

DDES and STVD Scheme with Adaptive Dissipation

To construct the DES-type RANS/LES hybrid methods based on SST model (Menter, 1994), the length scale should be introduced in the destruction term in the turbulence kinetic energy (TKE) equation.

$$\frac{\partial(\rho k)}{\partial t} + \frac{\partial \rho u_j k}{\partial x_j} = \frac{\partial}{\partial x_j} \left((\mu + \sigma_k \mu_t) \frac{\partial k}{\partial x_j} \right) + \tau_{ij} S_{ij} - \beta^* \rho k \omega \cdot F_{DES} \quad (1)$$

where $F_{DES} = \max \left[(1 - F_{SST}) \cdot \frac{L_t}{C_{DES} \Delta}, 1 \right]$ and the turbulence length scale is defined as $L_t = k^{1/2} / (\beta^* \omega)$; $C_{DES} = F_1 \times C_{DES, k-\omega} + (1 - F_1) \times C_{DES, k-\epsilon}$. F_{SST} is taken as function F_2 . Both F_1 and F_2 are two blending functions in SST model.

If $F_{SST} = 0$, the hybrid method reverts to a Strelets-type (Strelets, 2001) DES method. If $F_{SST} = F_2$, this hybrid approach becomes the DDES. Due to the properties of F_2 , $(1 - F_{SST})$ approaches zero near the wall, the DDES will act in the RANS mode. Also, if $(1 - F_{SST})$ becomes one outside the boundary layer, DDES goes back to the original Strelets-type DES model. Thus, DDES can ensure itself to act in the RANS mode near the wall without the effects on the local clustered grid. In other words, DDES can delay the switching from RANS to LES near the wall due to the grid scales, especially the locally refined grids in the streamwise and spanwise directions for the complex configurations.

C_{DES} is one of the most important parameters in DDES and it should be recalibrated before implementation. Fig. 1 presents the DIT and recalibration of C_{DES} using our in-house code. It is found that the two branches are smaller than the original values. Then, $C_{DES} = F_1 \times 0.4 + (1 - F_1) \times 0.3$.

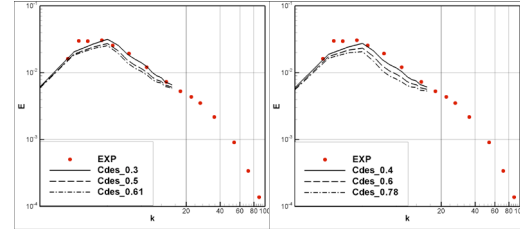


Fig. 1 DIT and C_{DES} recalibration ($k-\epsilon$ and $k-\omega$)

The spatial scheme for the convective terms of N-S equations is the symmetric total variant diminishing (STVD) scheme (Yee et al. 1998). The idea of STVD is to combine the high-order symmetric difference schemes with relatively lower-order dissipation terms to yield better accuracy. Because STVD is spatially symmetric, it has no inherent dissipation as does the upwind scheme. However, the symmetric scheme has dispersive errors. Then, this algorithm allows one to independently control the dispersion and dissipation errors in the solution.

$$F_{i+1/2} = \underbrace{F_{\text{symmetric}, i+1/2}}_{6^{\text{th}} \text{ order, symmetric, scheme}} - \underbrace{\phi \times \frac{1}{2} |\tilde{A}_{\text{inv}}| (q^R - q^L)}_{5^{\text{th}} \text{ order, WENO}} \quad (2)$$

where $F_{\text{symmetric}, i+1/2} = F_{i-2} - 8F_{i-1} + 37F_i + 37F_{i+1} - 8F_{i+2} + F_{i+3}/60$ and \tilde{A}_{inv} is the matrix of Roe. q^R and q^L are the primitive variables. For the original S6WENO5 scheme, the parameter ϕ is taken as one. In this paper, ϕ ranges from 0 to 1. Near the wall and in the irrotational region, ϕ approaches 1 and in the recirculation region, it is taken as 0. The distribution of ϕ is presented in Fig. 2 around TC. It almost performs as we hope.

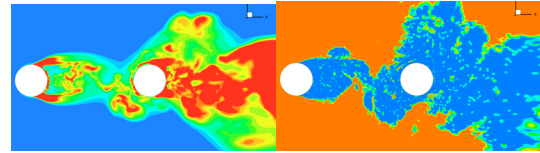


Fig. 2 Eddy viscosity and adaptive function distribution

OTHER NUMEIRCAL METHODS

Our in-house code of UNITS (Unsteady NavIer-Stokes equations solver), which is in a cell-central finite-volume formulation based on multi-block structured grids, is applied to validate the spatial schemes and turbulence modeling method. A modified fully implicit LU-SGS with Newton-like sub-iteration in pseudo time is taken as the time marching

method when solving the mean flow and the turbulence model equations. To obtain high temporal order, about 80 sub-iterations are applied to converge in a physical time step. The approach is in parallel algorithm using domain-decomposition and message-passing-interface strategies for the platform on PC clusters.

The TKE and specific dissipation rate transport equations are solved, decoupled with the mean flow equations using LU-SGS method with sub-iterations. The production terms are treated explicitly, lagged in time whereas the destruction and diffusion terms are treated implicitly (they are linearized and a term is brought to the left-hand-side of the equations). Treating the destruction terms implicitly helps increase the diagonal dominance of the left-hand-side matrix.

The computation of DDES starts from initial flow-fields by URANS. The time-averaged results are obtained after several relatively regular vortex-shedding periods.

RESULTS AND DISCUSSIONS

Unsteady and massively separated flows past NACA0021 and tandem cylinders are simulated using DDES with adaptive dissipation. The effects of spanwise length (SL) and QL assumption are discussed, respectively.

NACA0021 at Incidence of 60 Degrees. Due to the very large incidence, the flow becomes massively separated in the leeward side of the airfoil. The grids are locally clustering in the downstream region, shown in Fig. 3. In the X-Y plane, the overall grid points are about 20,000. Two SLs, 1 chord (C) including 41 points and 4C including 161 points, are used to study the effect of the SL.

The Mach number is 0.11 and the Reynolds number based on the chord is 2.7×10^5 . The angle of attack is 60 degrees. The non-dimensional time of each step is 0.02.

Histories of lift and drag coefficients (C_L and C_D) based on 4C case are presented in Fig. 4.

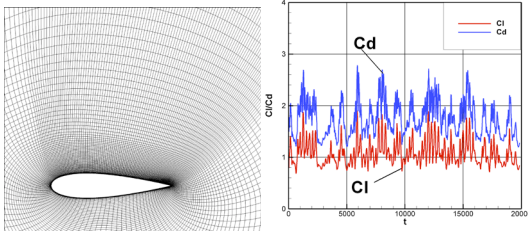


Fig. 3 Grids in X-Y plane Fig. 4 Histories of C_L and C_D

Table 1. Comparisons between computation and experiment

	C_L	C_D	1 st St.	2 nd St.
Exp.	0.931	1.517	0.20	0.40
1C	1.053	1.684	0.19	0.39
4C	0.908	1.428	0.19	0.40

In Table 1, the time-averaged lift and drag coefficients are compared with the measurements. At the same time, the

computations of first and second frequencies (St. number) also well match with the experiments. The SL is larger, the agreement is better.

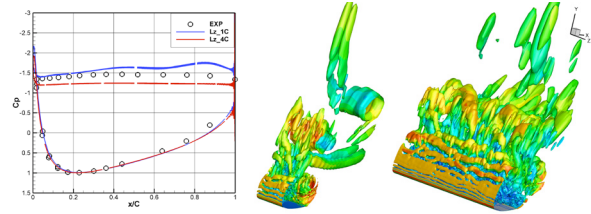


Fig.5 Comparisons on C_p and Q criterion

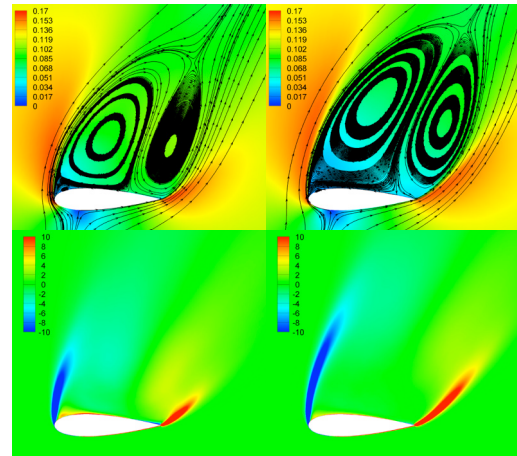


Fig.6 Streamlines and spanwise-vorticity of 1C and 4C

The comparisons on pressure coefficients (C_p) and Q are presented in Fig.5. On the windward surface, both SLs well predict C_p . The difference mainly focused on the leeward side. The SL is smaller, the agreement is worse. At the same time, the structures looks more abundant and the spanwise structures develop more sufficient when the SL is larger.

In Fig. 6, time-averaged flow patterns and spanwise vorticity are presented to compare the effect of the SL. Larger recirculation and longer shear layer near the leading and trailing edges are observed with larger SL.

After the analysis of time-averaged and instantaneous results, the SL has an important influence and it should be taken as large as possible.

Tandem-Cylinders with 3.7 Diameters Space. The tandem-cylinders is a prototype for interaction problems commonly encountered in airframe noise configurations (e.g., the oleo and hoses on a landing gear). The flow has been studied in a series of experiments performed in NASA Langley Research Center. Simulation of TCs can help testing the capability of turbulence modeling approaches, spatial and temporal methods to reproduce properly complex flow phenomena, such as the transition on the two cylinders,

separation of turbulent boundary layer, free shear layer instability, the interaction of unsteady wake from the front cylinder with the downstream one and unsteady massively separated flow between the cylinders and in the wake of the rear cylinder, etc.

In this article, fully turbulent (FT) and QL assumption are adopted to investigate the effect of fixed trip in experiment on the turbulent flow fields. As shown in Fig.7, the QL regions marked by red are similar with the experiment. The diameter of the cylinder is D and the space of two centers is $3.7D$.

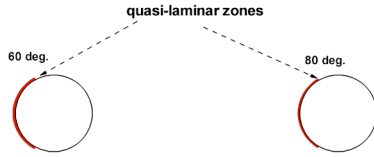


Fig. 7 Sketch map of TC and the quasi-laminar region

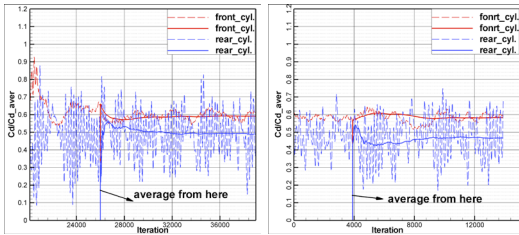


Fig. 8 The histories of C_D by DDES and DDES-QL

The velocity of freestream is 44m/s and the Reynolds number based on D is 1.66×10^5 , and the angle of attack is 0 degree. The mandatory grids in X-Y plane of ATAAC project are about $820,000$ and the spanwise length is $3D$ with 151 points. Then, the overall grids are about 12 million.

In Fig.8, the histories of drag coefficient by DDES and DDES-QL are demonstrated. DDES started from the flow fields by URANS, while DDES-QL started from the flow fields by DDES. The statistical time is smaller than the overall computational time, because the first a few periods are not suitable for averaging.

In Fig.9, C_p by two methods well match the experiments and differ little. On the windward surface of the front cylinder, $C_{p,rms}$ by DDES is a little larger than that by DDES-QL; however, on the leeward side of the front cylinder, it performs just reversely. On the windward surface of the rear cylinder, $C_{p,rms}$ by DDES looks almost the same with that by DDES-QL. On the leeward surface of the rear cylinder, $C_{p,rms}$ by DDES is a little larger than that by DDES-QL. It indicates that the QL assumption can slightly reduce the unsteadiness near the QL region, but it almost has no influence on the time-averaged C_p .

The streamwise velocity along the centerlines are presented in Fig.10. From this figure, the recirculation in the gap region by DDES-QL is a little smaller than that by DDES.

Despite the recirculation behind the rear cylinder by DDES-QL is a little larger than measurements with trip, it matches the measurements a little better. However, the recirculation behind the rear cylinder performs conversely. This phenomenon mainly results from the laminar region around the rear cylinder. The forced quasi-laminar region can reduce the turbulent intensity between the two cylinders and in the wake of the rear cylinder.

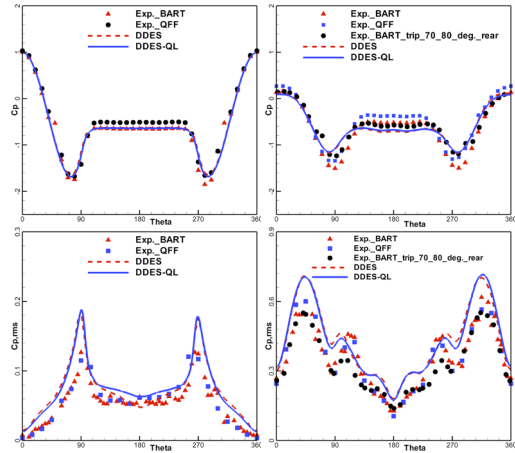


Fig.9 Comparisons on C_p and $C_{p,rms}$

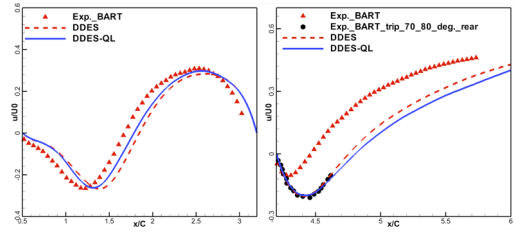


Fig.10 Comparisons on streamwise velocity at $y=0$

Because the periodic boundary condition is applied in the spanwise direction, the 2-D KTE is defined as $k = (u'^2 + v'^2) / (2U_{inf}^2)$ after eliminating the spanwise component.

From the comparisons on the contour of TKE shown in Fig.11, the TKEs by DDES and DDES-QL seem a little larger than the measurements without the trip on the rear cylinder. In the gap region, DDES and DDES-QL seems almost the same. Near the stagnation point on the rear cylinder, TKE by DDES-QL is a little smaller than that by DDES, but is still larger than that of experiments. In the wake, the TKEs are a little larger than experiments.

TKE at some typical sections are also used to explore the difference of DDES and DDES-QL. In the experiments, the TKE in the central line, where y is equal to 0 , can be applied to reflect the development and evolution of the flow.

In the gap region, computational TKEs are a little larger than the measurements, especially at $x/D=1.75$ and near the stagnation of the rear cylinder.

DDES-QL performs a little more reasonably than DDES in the wake, especially before $x/D=4.7$. DDES overestimate the TKE almost along the central line.

At two streamwise sections, where $x/D=1.5$ and 4.45 , TKEs by DDES and DDES-QL are compared with the measurements. At the first section, both DDES and DDES-QL overestimate the TKE. DDES-QL almost cannot reflect the QL assumption. The possible reasons are the long distance from the QL region on the front cylinder, which cause the decay of laminar disturbance. Fortunately, in the wake of the rear cylinder, DDES overestimate the KTE; while DDES-QL can well predict the KTE of measurements, especially the one that includes the trip on the rear cylinder.

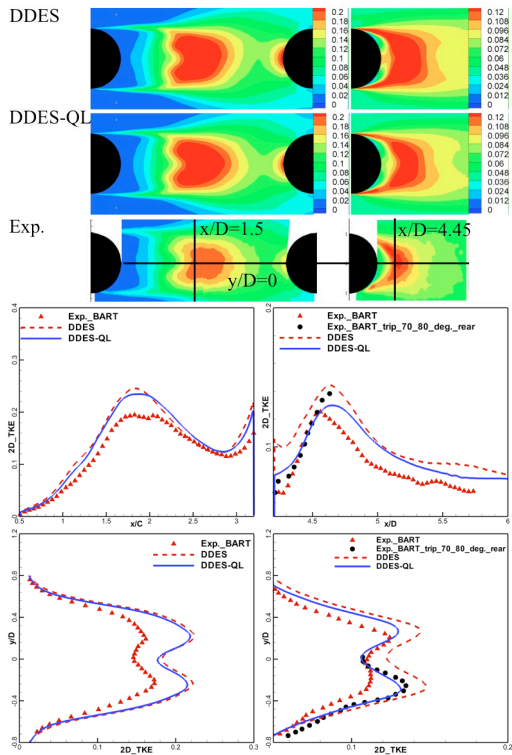


Fig.11 Comparisons on the turbulent kinetic energy

The pressure fluctuations at two samples are investigated, where one is 135 degrees on the front cylinder surface, and another is 45 degrees on the rear cylinder surface. After the analysis of fast Fourier transformation (FFT), we find that the pressure fluctuation at Point B is much larger than that of Point A. The main reason is that the front cylinder encounters the relatively “quiet” freestream flow, while the rear cylinder is always “washed” by the extremely unsteady wake detached from the front cylinder.

For Point B, both DDES and DDES-QL well predict the magnitude. The computational PSD by DDES is a 1 dB smaller than measurement without trip and is 1 dB larger than DDES-QL. The primary frequencies are the same with Point A and 12 Hz smaller than the experiments.

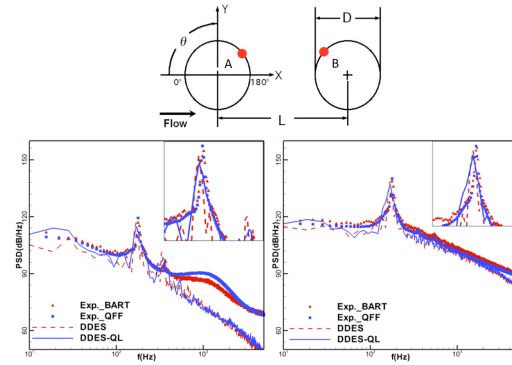


Fig. 12 Frequency and magnitude of pressure fluctuation at Point A (Left) and Point B (Right)

Table 2. Comparisons between computation and experiment

	Freq. of PA (Hz)	Mag. of PA (dB)	Freq. of PB (Hz)	Mag. of PB (dB)
Exp.	181	118	181	139
DDES	169	117	169	138
DDES-QL	169	115	169	137

For Point A, both DDES and DDES-QL under-predict the power spectra density (PSD) at the high frequency. The possible reason is that the shear layer after the front cylinder is too strong. The computational PSD by DDES is a 1 dB smaller than measurement without trip and is 2 dB larger than DDES-QL. The primary frequencies by DDES and DDES-QL are the same and they are 12 Hz smaller than measurements. The summaries of primary frequencies and magnitudes at Point A and Point B are listed in Table 2.

After analysis of time-averaged flow fields including C_p , $C_{p,rms}$, U , KTE, and so on, some instantaneous flow fields are presented to explore the features of the unsteady flow.

In Fig.13, the instantaneous spanwise vorticity of measurements and computations are compared. From the measurements, very small-scale turbulence structures are observed between the two cylinders and after the rear cylinder. It’s very difficult to accurately predict these small-scale structures using the URANS and DES-type with large dissipation scheme (Liu, 2010). Although the computational shear layer looks stronger than measurements, our DDES and DDES-QL with adaptive dissipation scheme can well capture the small-scale of structures successfully. The performances of DDES and DDES-QL look very similar.

In Fig.14, 3-D separated flow can be demonstrated using Q criterion. Because DDES and DDES-QL perform similarly, the iso-surface of Q criterion by DDES is only presented here. From this figure, we can find very complex flow phenomena, such as the shear layer instability, reattachment on the rear cylinder, wake after the rear cylinder, and so on.

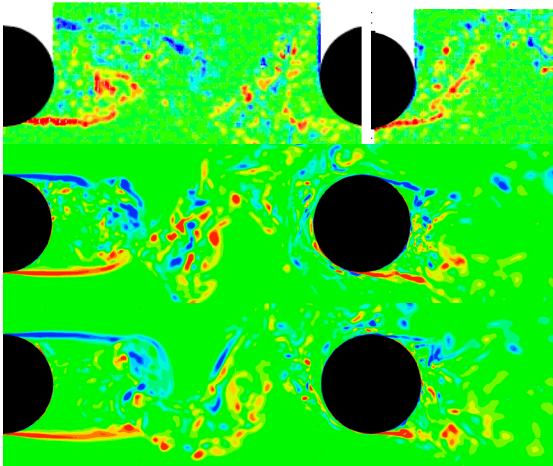


Fig.13 The comparisons on instantaneous spanwise vorticity (Exp., DDES and DDES-QL)

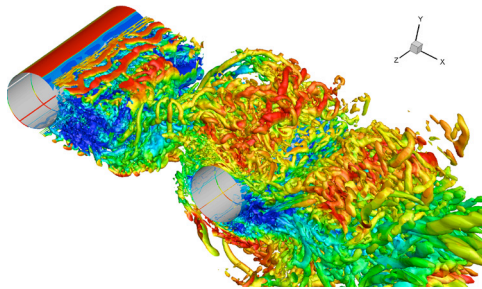


Fig.14 Instantaneous Q criterion by DDES

CONCLUSIONS

In this paper, unsteady flows with massive separation are predicted using DDES with adaptive dissipation. The important parameter, C_{DES} , in DDES is recalibrated using our in-house code. In the case of NACA0021 at incidence of 60 degrees, the effect of spanwise length is investigated and larger spanwise length is suggested to apply because the 3-D flow can fully develop. In the case of tandem cylinders, after analyzing the experimental data with and without the trip, we can find the trip has a great influence on the flow fields after the rear cylinder, such as the velocity, TKE and so on. In fact, the coefficients of $C_{P,rms}$ with trip are totally smaller than those without trip. DDES-QL performs more reasonably than DDES, especially when they are applied to predict TKE and streamwise velocity.

ACKNOWLEDGES

Part of this work was supported by EU project ATAAC (Contract No. ACP8-GA-2009-233710). It was also supported by National Science Foundation of China (Contract No. 11072129 and 10932005). The authors also thank Shanghai Supercomputer Center to provide computational resource.

REFERENCES

- Fu, S., Xiao, Z. X., Chen, H. X., Zhang, Y. F., and Huang, J. B., 2007, "Simulation of Wing-Body Junction Flows with Hybrid RANS/LES Methods," *International Journal of Heat and Fluid Flow*, Vol. 28, Issue 6, pp. 1379-1390.
- Haase W., Braza M., Revell A., 2009, "DESider - a European effort on hybrid RANS LES modeling". *Note on Numerical Fluid Mechanics and Multidisciplinary Design*, Vol.103.
- Jenkins, L. N., Khorrami, M. R., Choudhari, M. M., and McGinley, C. B., 2005, "Characterization of Unsteady Flow Structures around Tandem Cylinders for Component Interaction Studies in Airframe Noise," *AIAA Paper 2005-2812*.
- Jenkins, L.N., Neuhart, D.H., McGinley, C. B., Choudhari, M. M., and Khorrami, M. R., 2006, "Measurements of Unsteady Wake Interference between Tandem Cylinders," *AIAA paper 2006-3202*.
- Liu J., Xiao Z.X. and Fu S., 2010, "Unsteady flow around two tandem cylinders using advanced turbulence modelling methods", *International Computational Fluid Dynamics*, St. Peterburg, Russia.
- Menter, F.R., 1994, "Two-Equation Eddy-Viscosity Turbulence Models for Engineering Applications," *AIAA Journal*, Vol. 32, No. 8, pp. 1598-1605.
- Menter, F.R., and Kuntz, M., 2003, "A Zonal SST-DES Formulation," *DES-WORKSHOP*, St. Petersburg. (<http://cfd.me.umist.ac.uk/flomania/index2.html>)
- Neuhart, D.H., Jenkins, L. N., Choudhari, M. M., and Khorrami, M. R., 2009, "Measurements of the Flowfield Interaction Between Tandem Cylinders," *AIAA paper 2009-3275*.
- Spalart, P. R., Jou, W. H., Strelets, M., and Allmaras, S.R., 1997, "Comments on the Feasibility of LES for Wings, and on a Hybrid RANS/LES Approach," *First AFOSR International Conference on DNS/LES*, Ruston, LA. Advanced in DNS/LES, edited by Liu, C. and Liu, Z., Greyden Press, Columbus, OH.
- Spalart, P. R., 2000, "Strategies for Turbulence Modeling and Simulations," *International Journal of Heat and Fluid Flow*, Vol. 21, Issue 3, pp. 252-263.
- Strelets, M., 2001, "Detached Eddy Simulation of Massively Separated Flows," *AIAA paper 2001-0879*.
- Xiao, Z. X., Chen, H. X., Zhang, Y. F., Huang, J. B., and Fu, S., 2006, "Study of Delayed-Detached Eddy Simulation with Weakly Nonlinear Turbulence Model," *Journal of Aircraft* Vol. 43, No. 5, pp. 1377-1385.
- Xiao, Z. X., and Fu, S., 2009, "Studies of the Unsteady Supersonic Base Flows around Three Afterbodies," *ACTA Mechanica Sinica*, Vol. 25, pp. 471-479.
- Yee, H.C., Sandham, N.D., and Djomehri, M. J., 1998, "Low Dissipative High Order Shock-Capturing Methods Using Characteristic-Based Filters," *Journal of Computational Physics*, Vol. 150, Issue 1, pp. 199-238.